METEOROID FRAGMENTATION IN THE MARTIAN ATMOSPHERE AND THE FORMATION OF CRATER CLUSTERS E. L. Newland[1], G. S. Collins[1], S. McMullan[1], I. J. Daubar[2], N. A. Teanby[3], Katarina Miljković[4] and the InSight Science Team. [1]Department of Earth Science and Engineering, Imperial College, London, SW7 2AZ, United Kingdom (E-mail: eric.newland15@imperial.ac.uk); [2]Jet Propulsion Laboratory, California Institute of Technology, Pasadena, CA; [3]University of Bristol, UK; [4]Curtin University, Australia.

Introduction: NASA's InSight mission aims to determine an accurate estimate of the current impact rate on Mars and constrain internal structure using seismology. The detection of seismic waves generated by m-scale impactors, could play a vital role in achieving both objectives [1]. However, about 50% of such impactors form crater clusters as a result of meteoroid fragmentation in Mars' atmosphere [2], which greatly complicates seismic wave generation and efforts to relate crater properties to those of the initial impactor. Here we show that a recently-proposed model of meteoroid fragmentation that accounts for heterogeneous internal strength [3] does a good job of replicating the characteristic size-frequency and spatial distributions of crater clusters, while classical models of meteoroid fragmentation [4] are unable to match observations.

Martian Crater Clusters: For comparison with numerical model results, we analysed the size-frequency and spatial distribution of craters within 77 recently formed crater clusters on Mars [5]. As the effective diameter of the cluster ($D_{\text{eff}} = \sqrt[3]{\Sigma_{i=1}^{n} D_i^3}$) increases, the size-frequency distribution of craters in the cluster tends to become one dominated by a small number of large craters surrounded by numerous small craters. This observation can be quantified by the fraction of craters in the cluster that have a diameter larger than half the maximum crater diameter $F(> D_{\text{half}})$ (Fig 1). In addition, the aspect ratio of best-fitting ellipses to the spatial distribution of craters in the cluster display a large variation at small effective diameters and tend towards a circular shape at larger effective diameters.

Fragmentation models: To model the fragmentation of metre-sized meteoroids and formation of crater clusters on Mars we applied two different approaches: the classical Separated Fragments Model [4, 6, 7] (SFM) and the multi-component Fragment Cloud Model [3] (mcFCM), which was recently used to replicate energy deposition curves of a number of well-documented terrestrial fireballs formed by m-scale impactors. In both models, the motion and ablation of the meteoroid is described by the integration of standard meteor physics equations [8]. Meteoroid fragmentation is assumed to occur when the ram pressure on the meteoroid exceeds its internal strength ($\rho_a v^2 > \sigma_0$). In the SFM, the initial meteoroid is assumed to have uniform internal structure and when the initial strength of the object is exceeded, it separates into

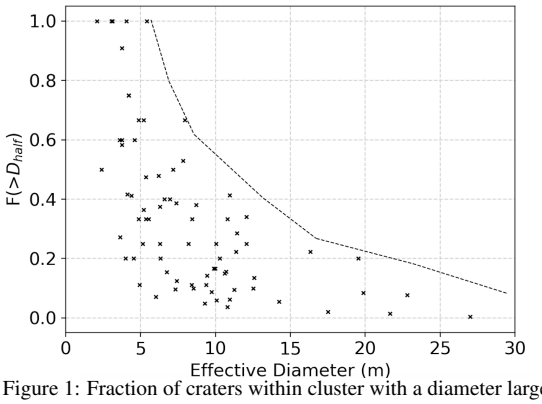

Figure 1: Fraction of craters within cluster with a diameter larger than D_{half} as a function of effective diameter for Martian data. Dashed line used for qualitative comparison with model results.

two child fragments (Fig 2a) with a lateral separation velocity, v_L [4] and with elevated strength σ_i owing to their smaller mass and assumed Weibull flaw distribution. The child fragments are able to undergo further fragmentation, when $\rho_a v^2 > \sigma_i$, resulting in an additional separation velocity and a further increase in fragment strength. The products of fragmentation are tracked until they are totally ablated or impact the surface. On impact an upper and lower bound of crater size is calculated using strength-regime crater-scaling relationships appropriate for non-porous and porous targets on Mars [9], respectively, as well as the lateral position of each crater.

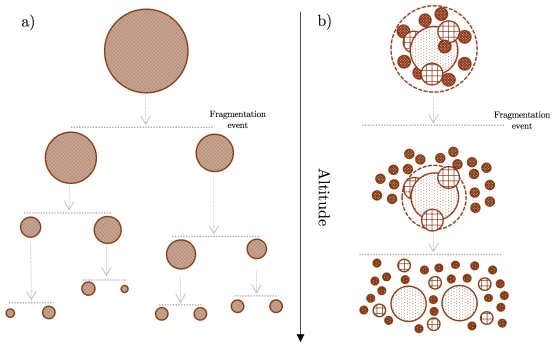

Figure 2: Schematic comparison of (a) the Separate Fragment Model (SFM) and (b) the multi-component Fragment Cloud Model (mcFCM).

The mcFCM differs from the SFM in two important ways. First, the mcFCM treats the initial meteoroid as a multi-component object comprising different structural groups with different initial strengths [3]. The most frag-

ile component will break off and begin fragmentation at the highest altitude; the most resilient component will begin to break up closest to the surface. Second, during each fragmentation event a cloud of fine debris is produced in addition to the two child fragments. The debris cloud plays no role in crater cluster formation, but has a substantial influence on the efficiency of energy transfer from the meteoroid to the atmosphere. In our implementation of the mcFCM, we consider three structural groups of equal mass, but with different initial strengths and fragment sizes. In the model presented here, the number of fragments in each group follows a ratio 1:3:9. Based on calibration of the mcFCM against terrestrial fireball data [3], we assumed an inverse correlation between initial fragment size and initial strength, such that the single-fragment component was always the strongest. When the strength of a structural group is exceeded, each fragment in the group simultaneously separates from the initial body with its own lateral velocity, v_L [4]; at the same time, each initial fragment undergoes break-up to produce two child fragments, with increased strength as per the SFM, in addition to a debris cloud. The child fragments are subject to a lateral separation velocity, v_L, and are able to undergo further fragmentation.

Results: Monte Carlo simulations were performed using the SFM and mcFCM with the same parameter probability distributions. Model parameters with unknown probability functions were assigned uniform probability distributions within upper and lower bounds. Based on 1000 modelled crater clusters (Fig. 3), the mcFCM results are remarkably consistent with the observed characteristics of martian crater clusters, while the SFM results are frequently inconsistent. The mcFCM results replicate the observed trend that as effective diameter increases the crater clusters become dominated by clusters consisting of a small number of large craters and numerous small craters (Fig 3). The mcFCM results also replicate the trend of large clusters forming in near-circular distributions whereas smaller clusters exhibit a range of planform aspect ratios. In comparison, the SFM results show no correlation between $F(> D_{\text{half}})$ and effective diameter. Moreover, a significantly larger proportion of crater clusters form with a $F(> D_{\text{half}}) = 1$, where all craters are of a similar size, which is not observed on Mars.

Discussion: The success of the mcFCM at replicating observed martian crater clusters, in comparison with the traditional SFM, suggests that accounting for multiple components of differing strength within the meteoroid is crucial for accurately modelling atmospheric disruption. The SFM considers a uniform initial body, which on fragmentation produces two similar-sized child fragments (Fig 2a) that are always stronger than their parent. Larger fragments are always weaker than smaller fragments and therefore more prone to further break-up events. This frequently leads to a final set of fragments all of similar size. In contrast, by allowing for structural components of different strengths, including some large strong fragments, the mcFCM encourages the production of a broader range of fragment sizes (Fig 2b) that produce crater clusters much more consistent with observations. Our successful models of martian crater clusters will allow improved estimates of impactor properties to be derived from observations of clusters detectable by InSight.

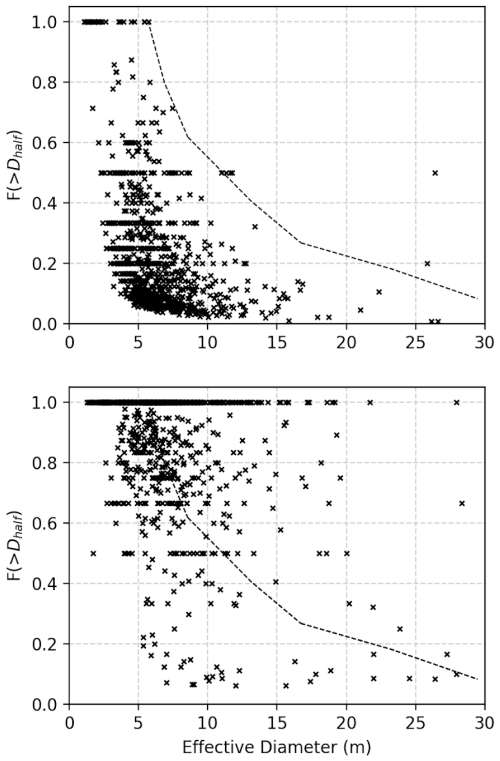

Figure 3: $F(> D_{\text{half}})$ as a function of effective diameter for the mcFCM (Top) and SFM (Bottom). Dashed line from Fig. 1 allows comparison with Mars observations.

Acknowledgments: GSC acknowledges support from UK Space Agency grant ST/S001514/1.

References: [1] Teanby, N. A. (2015) *Icarus*, 256:49–62. [2] Daubar, I. J. et al. (2013) *Icarus*, 225:506–516. [3] Wheeler, L. F. et al. (2018) *Icarus*, 315:79–91. [4] Passey, Q. R. & Melosh, H. J. (1980) *Icarus*, 42:211–233. [5] Daubar I. J., B. M.S. N. (2019) *JGR Planets, in review*, [6] Artemieva, N. A. & Shuvalov, V. V. (2001) *Journal of Geophysical Research E: Planets*, 106:3297–3309. [7] Popova, O. P. et al. (2007) *Icarus*, 190:50–73. [8] Öpik, E. J. & Singer, S. F. (1959) *Physics Today*, 12:54. [9] Holsapple, K. A. (1993) *International Journal of Impact Engineering*, 5:343–355.